Technology Maturation Efforts for the Next Generation of Grating Spectrometer Hyperspectral Infrared Sounders

Thomas S. Pagano, Dean L. Johnson, James P. McGuire, Mark A. Schwochert, and David Z. Ting, *Senior Member, IEEE*

***Abstract*—As we look forward to the next generation of hyperspectral infrared (IR) atmospheric sounders, grating spectrometers hold promise for improved performance (e.g., horizontal and spectral resolutions) and more rapid revisit while reducing the size and complexity of the instrument. We briefly revisit the technology used in the Atmospheric Infrared Sounder (AIRS), recognizing that it was developed in the 1990's and has matured key technologies in the areas of IR detectors, optical coatings, gratings, and cryocoolers. AIRS has been an unqualified success not only as a science and operational mission but also as a technology demonstration of the reliability and simplicity of grating spectrometer IR sounding instruments. Advancements in focal plane arrays (FPAs) have enabled a new class of grating spectrometer IR sounders that offer more spectral channels on a single FPA, mitigating some of the issues seen in AIRS that used linear arrays. These improvements have been manifested in the CubeSat Infrared Atmospheric Sounder (CIRAS) brassboard instrument, developed at the California Institute of Technology Jet Propulsion Laboratory with industry partner Ball Aerospace. Further enhancements beyond those used in CIRAS enable the development of a new class of instruments with a very long-wavelength infrared response and a very high spatial resolution (<2 km) that can be used for the next generation of IR sounders. Grating spectrometers provide advantages over other methods, including smaller apertures due to the ability to use larger FPAs, having no moving parts or laser metrology systems to produce spectra, lower internal FPA readout rates, and lower overall system data rates.**

***Index Terms*—Atmospheric, cryocooler, CubeSat, detector, focal plane array, grating, infrared, readout, SmallSat, sounder, spectrometer, technology.**

I. Introduction

INFRARED (IR) sounders operating in space today include the Atmospheric Infrared Sounder (AIRS) on the NASA Aqua satellite [1], the Cross-Track Infrared Sounder (CrIS) on the NASA/NOAA Suomi National Polar-Orbiting Partnership and NOAA Joint Polar Satellite System satellites [2], the Infrared Atmospheric Sounding Interferometer (IASI) on the EUMETSAT MetOp satellites [3], the Hyperspectral Infrared Atmospheric Sounder (HIRAS) on the CMA FY-3 satellites [4], the Geostationary Interferometric IR Sounder on the CMA FY-4A satellite [5], and the advanced IR sounder IKFS-2 on the Russian Meteor-M satellite [6]. All of these instruments are "hyperspectral," having very high spectral resolution ($\lambda/\Delta\lambda > 1000$) enabling the resolution of CO_2 and H_2O absorption features to make temperature and water vapor profiles for use by weather forecasters, meteorologists, and scientists worldwide. Advancements in wide-field optics, large-format focal plane arrays (FPAs), and cryocoolers offer enhanced capabilities to grating spectrometers that are well suited to IR sounders. This technology enables higher spatial and spectral resolutions and better operability and fidelity in a significantly smaller and simpler instrument than what was achieved in the past.

The AIRS approach to IR spectroscopy was motivated by the desire to have no moving or active parts (e.g., lasers) in the system to achieve a long-lifetime instrument. After over 20 years of operation in space, the AIRS grating spectrometer continues to produce spectra, and no major failures have occurred in the instrument. AIRS use of a grating spectrometer was ambitious at the time (mid 1990s) since the availability of IR detectors in the form of long (>100 pixels) linear arrays hybridized to readout integrated circuits (ROICs) was at its advent. The AIRS project worked with the industry to develop longwave IR cutoff HgCdTe detector materials, ROICs, multilinear array cryogenic packaging, cryogenic refrigerators (cryocoolers), and Dewar technology, not only to support the AIRS but also to advance these technologies for all IR programs nationwide. The project also supported optical component development, including gratings, optical coatings, and materials technology.

The availability of large-format IR FPAs brings advantages not available to AIRS to the next generation of hyperspectral IR grating spectrometer sounders. In particular, the push to achieve higher spatial and spectral resolutions in the next generation of IR sounders demands the use of larger FPAs and smaller detectors.

The signal collected by a grating IR sounder is the product of the etendue, the $A\Omega$ product, and the integration time. Etendue is also known as the product of the aperture area and the instantaneous field of view (IFOV) squared, where the IFOV is defined as the footprint size on the ground divided by the orbit altitude. Equivalently, the etendue can be defined as the product

Manuscript received January 14, 2022; revised March 11, 2022; accepted March 30, 2022. Date of publication April 8, 2022; date of current version April 26, 2022. This work was supported by National Aeronautics and Space Administration. (*Corresponding author: Thomas S. Pagano.*)

The authors are with the Jet Propulsion Laboratory, California Institute of Technology, Pasadena, CA 91109 USA (e-mail: tpagano@jpl.nasa.gov; dean.l.johnson@jpl.nasa.gov; james.p.mcguire@jpl.nasa.gov; mark.a.schwochert@jpl.nasa.gov; david.z.ting@jpl.nasa.gov).

Digital Object Identifier 10.1109/JSTARS.2022.3165168

of the detector area for a given footprint and the optics solid angle ($\sim\pi/4f\#^2$). For a given signal-to-noise ratio (SNR), one can trade etendue and integration time. For scanning systems, a larger FPA size will increase the field of regard (FOR), defined as the angular extent viewed by the entire FPA in the spatial dimension(s), leading to longer integration times since more area is viewed at any given instant. This increase in the integration time can be traded for a smaller aperture size for a given IFOV or a smaller footprint for a given aperture size.

The benefits of large-format FPAs for IR sounders have been demonstrated in the CubeSat Infrared Atmospheric Sounder (CIRAS) brassboard prototype IR sounder. CIRAS incorporates a wide-field all-refractive immersion grating spectrometer and a 512 $\times$ 640 element FPA that operates in the midwave IR (MWIR) and fits in a 6U CubeSat volume. (*Note:* We refer to the CIRAS FPA format as "large," although much larger formats exist today.) Results from testing of the brassboard show that CIRAS can achieve the required spatial, spectral, and radiometric performance for a lower-tropospheric temperature and water vapor sounder. The design approach using wide-field optics and large-format focal planes also applies to future, potentially larger than CIRAS, and more capable IR sounders that are predicted to be significantly smaller and lighter than legacy systems.

Future applications of IR sounders for weather forecasting and science investigations in the next two decades by the USA include the next generation of LEO and GEO IR sounders for NOAA and various missions relating to atmospheric winds and the planetary boundary layer for NASA Earth Sciences [7]. Assurance of core capabilities and compatibility with stable budgets are the top two strategic objectives identified in the NOAA Satellite Observing Systems Architecture (NSOSA) study [8]. The study identifies IR sounders as "likely to achieve significant reductions in size, weight, and power" and suitable for technology insertion into the future observing system architecture. Regional real-time IR soundings (from GEO) ranked number 31 on the NOAA prioritized list of 44 measurements but recently have become a priority for NOAA as part of their GEO-XO program [9]. For the "hybrid" architecture, the NSOSA study recommends disaggregation of satellites and consideration of global 3-D winds from a cluster of high-resolution sounding small satellites. The NSOSA study also recommends future systems that include high spatial resolution sounding capabilities in a single orbit. Grating spectrometer sounders address these recommendations by offering compact configurations like CIRAS to reduce the cost of multiple satellites in the formation to measure 3-D atmospheric motion vector (AMV) winds while offering high spatial resolution with modest data rates from LEO in a CubeSat volume. Studies referred to below show that grating spectrometer sounders can meet the next generation of LEO and GEO operational requirements by offering high performance, low risk, long life, and high accuracy in a compact package.

II. AIRS on Aqua

The AIRS on the EOS Aqua Spacecraft (see Fig. 1) was launched on May 4, 2002, and it is still functioning as well as it did the day it was first claimed operational. The AIRS is a "facility" instrument developed by NASA as an experimental

Fig. 1. Atmospheric IR sounder.

demonstration of advanced technology for remote sensing and the benefits of high-resolution IR spectra to weather forecasting and science investigations. The AIRS was designed to measure temperature and water vapor profiles with accuracies comparable to radiosondes, granted with a lower vertical resolution but offered with global daily coverage.

The data from AIRS are assimilated into numerical weather prediction (NWP) models and have demonstrated among the highest forecast improvement of all data types assimilated. The data are regularly used in studies of processes affecting weather [10] and climate [11]. The data are also used in applications including volcano alerts [12], drought prediction [13], and ozone chemistry [14]. The AIRS instrument has shown exceptional radiometric stability to date, making it a valuable tool for climate trending and model validation [15].

A. AIRS Technology

The AIRS instrument, developed by BAE Systems Inc., incorporates numerous advances in IR sensing technology to achieve a high level of measurement sensitivity, precision, and accuracy [16]. During the timeframe of the AIRS development, technology maturation was often performed as part of the flight instrument program. Fig. 2, the first column, shows a few of the technologies that matured during the AIRS development, including a multiple afocal-relay all-reflective grating spectrometer, long-wavelength cutoff HgCdTe photovoltaic IR detectors, and dual-pulse tube cryocoolers. These are the core technologies that we examine here and the development of which JPL and industry have contributed over the years, in the context of IR sounding.

Although the AIRS instrument has been well documented, a few key points regarding the AIRS design are worth highlighting. The spectrometer has no moving or active parts and requires minimal signal processing to make calibrated spectra. Frequency determination is based on preflight measurements, but the final "climate quality" determination of frequency comes from fits of modeled spectra to the observed spectrum on-orbit [17] and resampled to a common grid for the mission in the final radiance product. The entire optical system was novel at the time, providing pupil imaging in order to provide a uniform spatial response, but the key technical challenges were the development of the FPAs, grating, and optical filters. The long-wavelength

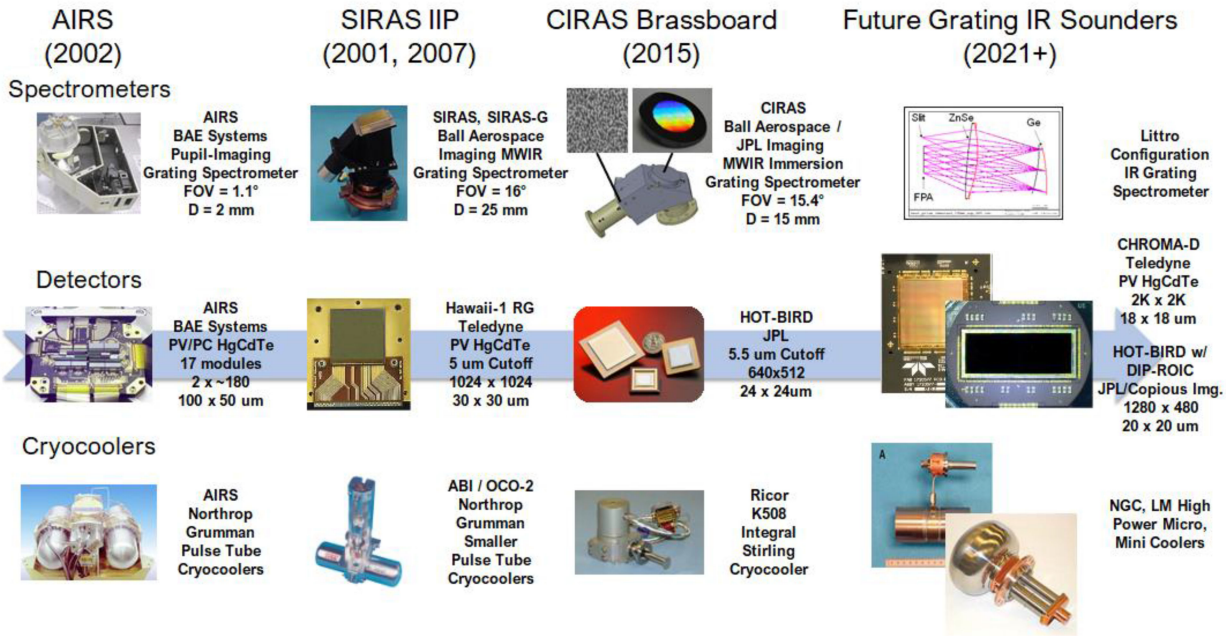

Fig. 2. Technology evolution of IR grating spectrometer IR sounders at JPL and industry and future technologies under consideration.

cutoff of PV HgCdTe was extended to 13.7 μm in the AIRS FPA and was a significant technology development success for the project. The AIRS detectors require operation at 58 K to minimize dark current to reduce noise and prevent ROIC saturation. Northrop Grumman Space Systems developed the pulse tube coolers for the AIRS instrument [18]. Despite having two cryocoolers running simultaneously, the AIRS does not suffer from vibration sensitivity since the grating spectrometer acquires all spectral channels simultaneously in 22.4 ms.

B. AIRS Performance

The AIRS has exceptional radiometric and spectral sensitivity and stability [19], [20] and has been operational from its launch in 2002 to the present without a serious failure. The radiometric stability is better than 2–3 mK/year [21] with accuracies better than 250 mK [22]. The AIRS performance has been well documented, and the instrument performance has not changed over the 20-year record, so we refer the reader to the literature [23]. Instead, we address concerns with the AIRS performance that have been raised as a basis for claiming fundamental issues with grating spectrometers for future IR sounders [24]. Recognizing that AIRS was a technology development program for IR sounders (including long-wave cutoff HgCdTe) its performance cannot be scored against instruments developed almost 10 years later, regardless of the technology differences. Instrument artifacts seen in AIRS are particular to the AIRS implementation and have been corrected, for the most part, in the AIRS Level 1C product [25]. The three major concerns expressed include the following.

1) Spectral Stability: Spectral stability of AIRS in terms of positional accuracy at the focal plane is less than 2 μm over the mission or 20 ppm of the center frequency. Changes of this magnitude have not been seen to significantly impact the L2 data products but must be accounted for in climate trending. By analyzing upwelling spectra, scientists determine the AIRS center frequencies to be better than 1 ppm, including Doppler corrections [17]. The process of fitting to the upwelling spectra is also performed automatically in the AIRS level 1B product to about 5 ppm or better. Knowledge of the frequencies is used to correct the orbital and secular drift of the AIRS spectra in the Level 1C product by resampling the spectra to a common grid for the mission. This methodology works well for AIRS and can be used as a model for future grating spectrometer IR sounding instruments.

2) Intraspectral Artifacts Related to Spatial and Spectral Response Differences: AIRS used pupil imaging in an attempt to reduce spatial variability among channels in the spectrum and distribute the scene energy across the 17 individual modules of a relatively large focal plane. This worked well for most channels; however, a few channels near the ends of modules can see coregistration differences exceeding 20% in many channels, most likely due to vignetting in the optical train (see Fig. 3). These channels are only impacted in high spatial contrast scenes (about 2% of all scenes) and are corrected in the AIRS Level 1C data product through the replacement of the offending channels with their PC reconstruction. A technique using an independent data set has been demonstrated using MODIS to remove these artifacts [26]. The figure also shows the performance of the CIRAS instrument brassboard prior to any correction, showing that these artifacts are not present.

3) Spectral Normalization Among Multiple Instruments: This is not necessarily a problem with the AIRS instrument itself, whereas it is claimed as a fundamental issue with grating spectrometers. In a grating spectrometer, to first order, the spectral response function (SRF) is the product of the convolution

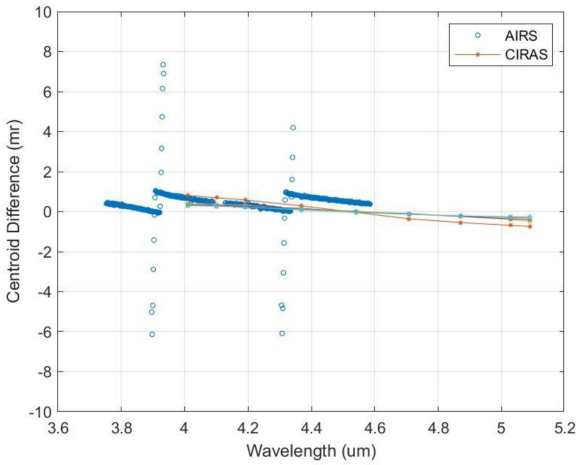

Fig. 3. Azimuth centroid difference for AIRS and CIRAS. CIRAS does not show the large centroid differences at the ends of the array.

of the entrance slit, optical blur, and detector angular response functions with the angular dispersion of the grating ($d\lambda/d\theta$). Each instrument's SRF will be different to the extent that the design and alignment are different. NWP centers and retrieval scientists utilize these SRFs in their radiative transfer models (RTMs) to assimilate multiple instrument types today with great success (e.g., AIRS, CrIS, and IASI). In future IR sounders, and as demonstrated in CIRAS, the SRFs can also be determined accurately and made similar, to the extent possible, in a constellation, whereas the center frequencies can be resampled to a common grid. If necessary, SRFs for each individual instrument can be used in the RTMs. The cost is a one-time computation on the ground to enable the RTM to be called for the particular instrument. The cost of this in an FTS is the large degree of oversampling during the dwell time in order to generate an interferogram. We will discuss this more below.

One additional problem identified with AIRS is the loss of spectral channels where both the primary and redundant detectors have gone out. Future grating spectrometers IR sounders like CIRAS will have several spatial pixels (detectors) per horizontal resolution element (11–42 in CIRAS) enabling 100% yield in the spectrum.

III. CubeSat Infrared Atmospheric Sounder

A. Background

In the early 2000s, JPL and Ball Aerospace matured technologies for a Spaceborne Infrared Atmospheric Sounder (SIRAS) under the NASA Earth Science Technology Office (ESTO) Instrument Incubator Program (IIP). Technology matured on these programs is shown in Fig. 2, column 2, and includes a demonstration of a wide-field very long-wavelength infrared (VLWIR; $\lambda c > 13$ μm) grating spectrometer operating from 12 to 15.4 μm with a spectral resolution of about 0.7 cm^{-1} that used an AIRS linear array [27]. Later, the SIRAS-G IIP prototyped a GEO IR sounder and used an MWIR all-refractive grating spectrometer operating from 3.3 to 4.8 μm with a spectral resolution of about 1.4 cm^{-1}. SIRAS-G used a 1K $\times$ 1K Teledyne H2RG focal plane [28]. These efforts formed the foundation of the wide-field all-refractive large FPA grating spectrometer concept.

In 2013, the Office of Systems Development at NOAA commissioned JPL to perform a study to examine current and future requirements for meteorological imaging and sounding and the impact of these requirements on instrument resource requirements and cost, given technology advancements in the last decade. The technologies studied were similar to SIRAS but with later optical and FPA technology, particularly the Teledyne CHROMA FPA shown in Fig. 2, column 2. The study showed that a single instrument, called the Moderate Resolution Infrared Imaging Sounder (MIRIS) [29], could be designed to meet the majority of the imaging requirements of the Visible Infrared Imaging Radiometer Suite (VIIRS) and the sounding requirements of CrIS simultaneously but at 2 km horizontal resolution from LEO. Recent updates to the MIRIS radiometric model show that by including a linear variable filter (LVF) or "Wedge" filter at the FPA and updating detector performance estimates, the NEdT requirement of 0.2 K can be met at all wavelengths.

In 2015, the NOAA Office of Products Planning and Analysis (OPPA) contracted JPL to perform a study of the technical feasibility of developing an IR temperature and water vapor sounder in a CubeSat volume. It was recognized that there could be reduced capability compared to the current operational sounder (CrIS), but demonstrating that a very low-cost option for an IR sounder that would meet "Threshold" capability was important to NOAA at the time and is currently within the NOAA trade space for future architectures [30]. The JPL study for NOAA demonstrated that an IR temperature and water vapor sounding payload, the Earth Observing NanoSatellite-Infrared (EON-IR) operating only in the MWIR, with 625 channels from 4.08 to 5.13 μm, complete with a scan mirror, a grating spectrometer, an Integrated Detector and Cryocooler Assembly (IDCA), and electronics could be packaged in a 6U spacecraft using technology available at the time [31].

There was some concern over using only the temperature and water vapor sounding features in the MWIR. Independent studies were performed that predicted that assimilation of CIRAS into the forecast system has a generally positive impact, with the control being all operational observations available to the GDAS/GFS in the January 2015 implementation in one study [32], and when added at new times of day compared to the CrIS [33] in another.

Later that year, JPL was awarded a contract to build the CIRAS instrument as part of the In-Flight Validation of Earth Science Technologies (InVEST) program sponsored by the NASA ESTO [34], [35]. After one year of development, the program was canceled due to projected cost overruns to develop a flight system; nevertheless, much progress was made, including the fabrication of the FPAs. In 2018, NOAA OPPA sponsored the completion of the optics assembly shown schematically in Fig. 2, column 3. The NOAA sponsorship enabled completion of a brassboard of the CIRAS instrument and ambient performance testing, allowing Technology Readiness Level (TRL) 4 of the instrument to be achieved [36]. More recently, the CIRAS

TABLE I
AIRS PERFORMANCE AND CIRAS EXPECTED PERFORMANCE AS DEMONSTRATED BY THE BRASSBOARD UNIT FOR A 600-KM ORBIT

Parameter	AIRS Performance	CIRAS Brassboard
Vertical Range	1000-<100mb	1000-400 mb
Temperature Accy	≤1.5 K/km	≤2.0 K/km
Humidity Accy @1000mb	15%/2km	20%/2km
Spectral Range	3.7-15.4μm	4.04-5.12μm
Spectral Resolution	≤0.5-2.2cm^{-1}	≤ 2-3 cm^{-1}
Spatial Res. (nadir)	13.5 km	3.5 km, 14 km
Scan Range	1750 km	265 km, 1521 km
NEdT	0.1-1.0K	<0.2K
Size	1.4x0.8x0.8m^3	4U (0.2x0.2x0.1m^3)
Mass	177 kg	4 kg
Power	256W	23 W

completed two cycles of thermal vacuum (TVac) preparatory tests, having performed exceptionally well. A third round of testing is planned for mid-2022, after which time results will be published. Performance results from the ambient testing are presented below (in Section III-E) and demonstrate compliance at the system level for most key performance parameters.

B. Instrument Concept

Table I shows the expected performance of the CIRAS compared to AIRS. CIRAS is designed to fit in a 4U volume of a 6U CubeSat. The system takes advantage of the ability to do both temperature and water vapor sounding in the MWIR in a single band ranging from about 4.08 to 5.13 μm with 640 channels and a spectral resolution of about 5 nm across the band. The resulting retrieval sensitivity for these products was calculated and is shown at the end of this section. The CIRAS 13.5 km spatial resolution is designed to match AIRS from a 600-km orbit, but it can be adjusted at any time in flight to achieve the same resolution for other LEO orbits. CIRAS can achieve a higher spatial resolution of up to 3.5 km by changing the pixel aggregation scheme, frame averaging, scan rate, and scan range.

Other products not listed in the table that CIRAS can potentially provide include lower tropospheric carbon monoxide and land surface temperature. Also, multiple IR sounders in a trailing orbit could be used to provide a time series of 3-D water vapor profiles, which could, in turn, be used to retrieve AMV winds [37], [38]. Retrieval of AMV winds from LEO is facilitated by a cost-effective instrument, like CIRAS, that can be hosted on a SmallSat or CubeSat and launched as a secondary payload.

A CAD illustration of the CIRAS instrument concept as conceived in the flight configuration is shown in Fig. 4. Energy from the Earth scene is directed to a refractive telescope using a gold-coated single-axis scan mirror mounted on a stepper motor. The scan mirror rotates 360° to view the Earth, cold space, and an internal blackbody for calibration. The blackbody is a simple flat plate composed of black silicon, heat sunk and instrumented with a temperature sensor to provide high emissivity and durability in a compact design. Energy from the telescope is focused onto the entrance slit of an all refractive MWIR grating spectrometer developed by Ball Aerospace, operating in first order, with an immersion grating and entrance slit made at JPL.

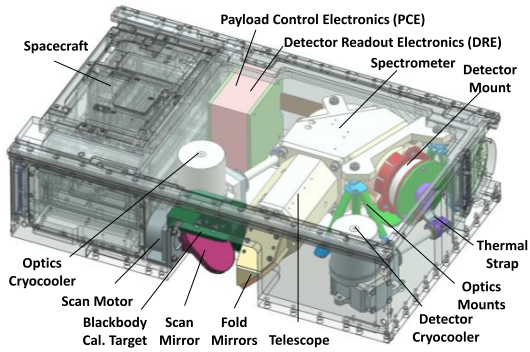

Fig. 4. CIRAS is designed to fit in a 6U spacecraft.

The telescope and spectrometer are cooled to 190 K using a Ricor K508N rotary Stirling cooler. The spectrometer disperses the energy across the spectral range and produces a 2-D image at the focal plane with one direction spatial and the other spectral. The detector array is based on the InAs/InAsSb type II strained layer superlattice IR absorber material incorporated into the high operating temperature barrier infrared detector (HOT-BIRD) device architecture developed at JPL [39], [40]. The HOT-BIRD detector arrays are hybridized with a Lockheed Martin Santa Barbara Focalplane (SBF) 193 ROIC to make an FPA. The FPA is packaged on a carrier and mounted with a cold shield and a two-band blocking filter. The filters reduce background flux and ghosting. The detector is cooled to 115 K using a second Ricor K508N cryocooler heat sunk to the spacecraft housing, which equilibrates at 308 K. The Payload Control Electronics provide control of the scanner, coolers, housekeeping, and communications with the spacecraft and detector readout electronics (DRE). The DRE provides clocks, biases and analog-to-digital conversion of the signals from the FPA. The brassboard uses the IDCA and DRE, developed by IRCameras, allowing testing in ambient. In the flight configuration, ICDA is not used; the detector mounts directly to the optics with a heat strap to the cryocooler, requiring the whole assembly to operate in TVac. The CIRAS is currently designed for a 6U or 12U CubeSat developed by Blue Canyon Technologies, but it can be easily accommodated by a variety of small spacecraft.

C. Method of Operation

The CIRAS employs a large-format FPA enabling a slow scan rate and uses the high density of pixels and frame averaging to achieve the desired size of the footprint. For example, in Fig. 5, for a 600-km orbit, the CIRAS telescope projects a slit onto the ground that is 12 footprints along-track (compared to 1 for AIRS). Again, the wider field of view produces a slow scan for a longer integration time, enabling a smaller aperture for a given SNR. On the image side of the slit, a collimator, identical to the telescope, collimates the image of the slit onto the grating. Light is reflected off the grating in the direction perpendicular to the slit according to its wavelength, producing a spectrum at the FPA (horizontally in the figure) when reimaged by the camera lenses. The image projected through the slit is only two detectors wide for a single wavelength when projected on the FPA.

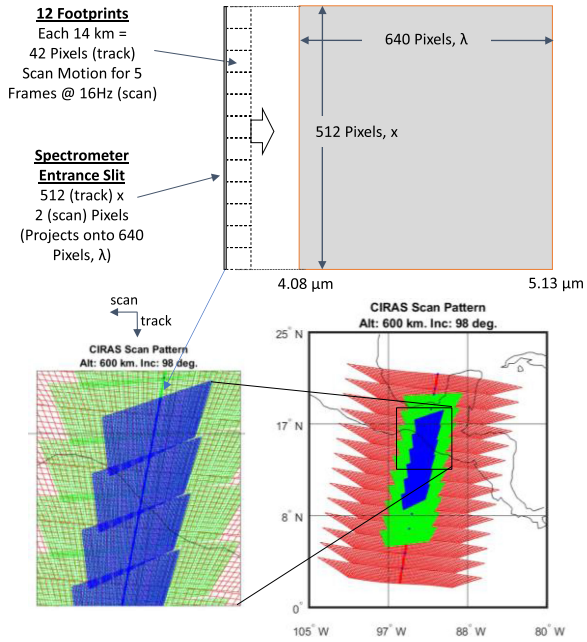

Fig. 5. (Top) Schematic of CIRAS pixel aggregation scheme for a 600-km orbit and 14 km spatial resolution. (Bottom) Resulting scan pattern as projected on the Earth for 14 km (Red), 7 km (Green), and 3.5 km (Blue).

TABLE II
CIRAS CAN ACHIEVE MULTIPLE SPATIAL RESOLUTIONS IN DIFFERENT MODES (ORBIT: 600 KM)

CIRAS Modes	Imaging	Zoom	Regional	Global
GSD (km)	1.0	3.5	7.0	14
Pixels	3	11	22	42
Channels	21	640	640	640
Swath (km)	386	265	561	1521
Data Rate (Mbps)	0.8	1.3	0.7	0.4

The motion of the scan mirror covers the appropriate distance by judicious choice of scan rate, frame rate, and the number of frames to add. The spatial information along the slit (vertically in the figure) in the along-track direction is preserved. The spatial resolution along-track is achieved by adding 42 pixels to make a single 14-km footprint. Higher spatial resolution is achieved by adding fewer pixels as shown in Table II and is limited by the focus and image quality of the optical system to the detector and is about 2–3 pixels or $<$1.8 mr. We can take advantage of the high spatial resolution imaging capability of CIRAS to achieve 1.0 km spatial resolution "Imaging" mode where we recover SNR by averaging 30 spectral channels, leaving about 21 spectral bands at this spatial resolution. All other modes produce 640 spectral channels. The swath width is reduced in higher spatial resolution modes to increase the dwell time to make up for lost SNR from coadding fewer pixels.

The FPA's nominal frame rate is 16.2 Hz, producing a data stream of 74.1 Mb/s at 14 bits/pixel. Five frames are averaged per dwell time (footprint) in Zoom, Regional, and Global modes and one frame in Imaging mode. The resulting data rate after frame averaging and along-track pixel binning is shown for each mode

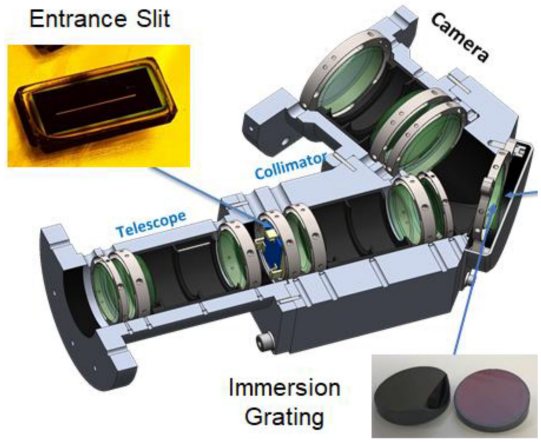

Fig. 6. CIRAS optomechanical design.

in Table II. Assuming a 6-min downlink at 3 Mb/s per orbit from the CubeSat (S-band), we can downlink 46% of the data in global mode and correspondingly less for the other modes without any compression. In an operational system requiring a 100% duty cycle, data compression or channel selection will be used to downlink the necessary data.

D. CIRAS Technology

The CIRAS represents an evolution over the AIRS type of grating spectrometer by allowing a much broader spectral range across a single FPA. This is now possible with new large-format FPAs offering one spectral channel per pixel, or 640 channels in the case of CIRAS. Since the optics are rotationally symmetric, the full FPA is imaged along the slit, offering a wide 15.4° field of view of the ground. In this section, we describe in a little more detail the optics, detectors, and cryocoolers used on CIRAS. These technologies were chosen for their simplicity, low cost, and high performance and were available at the time of the CIRAS design. Advancements have been made that show capability well beyond what we use in CIRAS. We touch on these in Section IV.

1) CIRAS Optics: The CIRAS optical system is remarkably simple but employs state-of-the-art optical manufacturing, assembly, and testing to achieve the desired level of performance in the IR. The optical system consists of the camera, the collimator, and the telescope, as shown in Fig. 6. The CIRAS telescope has a 15.0 mm aperture diameter and a 39.7 mm focal length, whereas the spectrometer camera has a 45.0 mm focal length. The basic approach using all refractive optics was developed by JPL and Ball Aerospace in the late 1990s and mid 2000s. There are no moving parts or lasers required for operation, and once assembled, the system produces an image of the slit and a spectrum for each position along the slit continuously, with no power or moving parts. Spectral calibration uses the upwelling spectrum or an on-board calibration target (e.g., parylene), and stability is achieved through temperature control, like on AIRS. The SIRAS and SIRAS-G IIPs demonstrated wide-field all-refractive grating spectrometer systems operating in the VLWIR and MWIR, respectively, with spectral resolution

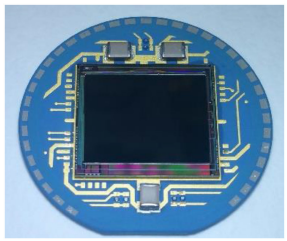

Fig. 7. CIRAS FPA mounted on a fanout board.

and field of view comparable to the CIRAS. CIRAS is different in that it employs a silicon immersion grating developed at JPL using e-beam technology. The immersion grating increases the dispersion by the grating according to the refractive index of the substrate and allows more favorable reflecting angles and an overall smaller spectrometer.

The slit is similar to those developed by JPL for the Orbiting Carbon Observatory 3 instrument [41], also a space-based grating spectrometer, and is darkened with black silicon. The required slit width is 2 pixels wide, and considering the magnification of the spectrometer of 0.88, this gives a required slit width of 42.2 μm. The measured slit width ranges from 40.0 to 45.0 μm, giving a parallelism of $+/-5\%$ with a mean width of 42.5 μm, meeting our requirements for parallelism for the technology demonstration.

All three optical subsystems, telescope, collimator, and camera, are very similar and composed of three refractive lenses each. The optical design model shows a worst-case smile of 30 μm and a keystone of 9.3 μm, better than our 2-pixel requirement of 48 μm. The materials used, i.e., silicon, germanium, and IRG-25 IR chalcogenide glass, were selected for their high index of refraction, good transmittance in the MWIR, and their thermo-optical properties. The CIRAS spectrometer has been designed to be athermal from ambient to the operational temperature of 190 K. This means that as the optics and spectrometer housing respond to change in temperature, the instrument remains in focus. Although the optics are temperature controlled to 190 K in the flight system, this feature allows the spectrometer to operate at ambient for performance validation as reported below.

A stray light model of the instrument was performed as part of the design. The model showed ghosting of signals due to reflections off the first surface of the immersion grating. To mitigate these effects, the grating was modified, and a two-band filter was placed at the focal plane, with a break at 4.6 μm. This had the added benefit of reducing the background flux at the detector. Other possible errors, including stray light and scatter, are controlled by the black silicon absorption of the entrance slit, baffles, and coatings within the optics and the e-beam control on the grating. Although performance characterization for ghosting, scatter, and stray light has not been performed, none was seen incidentally during the initial testing of the brassboard.

2) CIRAS Detectors and ROIC: Fig. 7 shows the CIRAS FPA mounted on the fanout board. CIRAS uses a 512 $\times$ 640 element, 24-μm pitch JPL HOT-BIRD array. The HOT-BIRD technology is based on III–V compound semiconductors and offers a breakthrough solution for the realization of lower dark current and improved uniformity and operability compared to II–VI material (HgCdTe) at lower cost [39], [40]. Low 1/*f* noise and high temporal stability allow CIRAS to use a slow scan for better sensitivity and less frequent calibrations. The ROIC chosen for the CIRAS FPA is the SBF193 by Lockheed Martin. Dozens of detectors hybridized to ROICs were successfully fabricated during the CIRAS InVEST effort on the first lot, demonstrating the high producibility of the fabrication process. The FPA selected for integration into the IDCA for the brassboard was tested at an operating temperature of 115 K and meets performance requirements as shown in Table III.

TABLE III
CIRAS HOT-BIRD FPA PERFORMANCE REQUIREMENTS AND OBSERVED VALUES

Detector	Requirement	Observed
Pixel Size (μm)	24±1	24
Spectral Range (μm)	4.08-5.13 μm	2-5.4 μm
QE @ 4.1 μm	>0.35	>0.4
Operability	>0.95	>0.999
Dark Current (A/cm^2)	<7.54e-07	<2e-07
Frame Rate (Hz)	30.0±10%	<88 (max)
ROIC Saturation (e-)	>8e+06	8.4e+06
ROIC Noise (e-)	<600	<500
Operating Temperature	<120K	115K

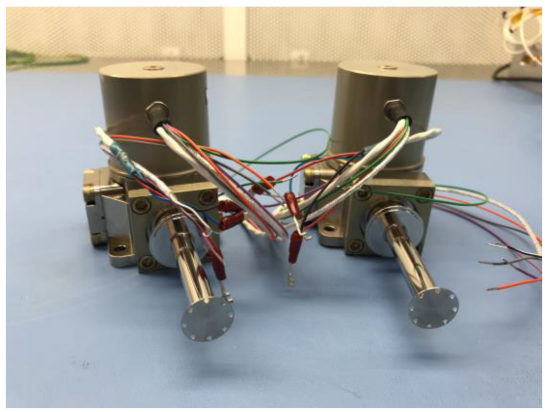

Fig. 8. CIRAS uses the Ricor K508N Stirling Cryocoolers.

3) CIRAS Cryocoolers: Two Ricor K508N Stirling cryocoolers (see Fig. 8), identical to the ones used in the IDCA (shown in Fig. 9), are planned for use to control the focal plane temperature to 115 K and the optics to 190 K. Ricor cryocoolers were chosen for their low cost and compact size. Other longer-life, compact cryocoolers can be considered for future operational versions. This cooler has a mean time to failure goal of 10 000 hours. Model analysis shows it will take about 50 h to cool the optics from a temperature of 300 to 190 K. The cooling margin for the optics cooler is 24%. It will take <1 h to cool the FPA from 293 to 115 K. The cooling margin for the FPA is 200%.

The heat from the cryocoolers, electronics, scan motor, and survival heaters will be conducted to the instrument panel that becomes one of the 2U $\times$ 3U panels of the 6U or 12U CubeSat. The entire spacecraft radiates the heat, achieving an operational

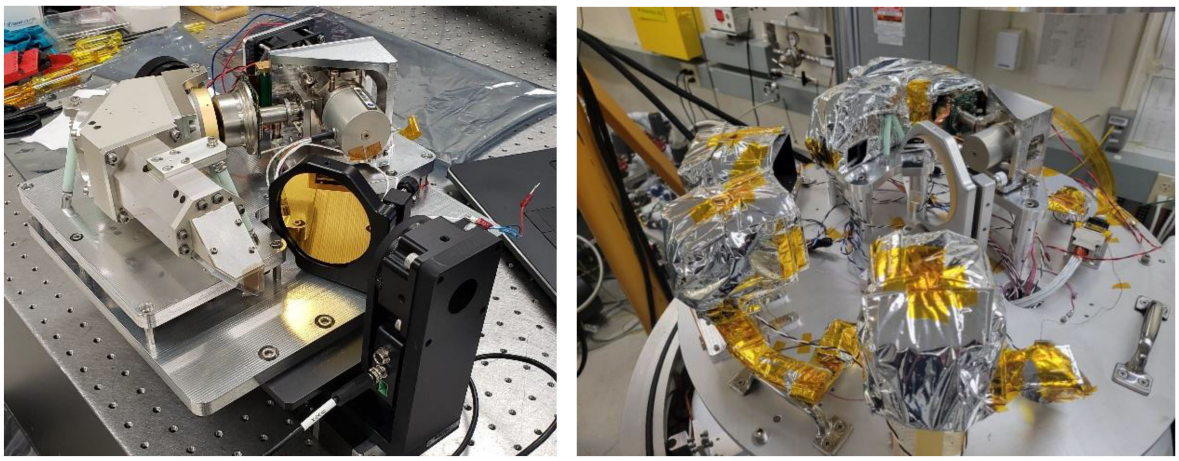

Fig. 9. CIRAS brassboard in ambient (left) mounted on a two-axis gimbal and stationary mirror and in TVac (right) with a GSE scan mirror viewing three blackbody targets.

temperature of nominally 308 K. This thermal architecture works with all beta angles and orbit altitudes from 200 km and higher. A sunsynchronous orbit is not required, and the thermal design is compatible with any orbit inclination. Survival heaters on the cryocooler and instrument electronics are included to maintain the equipment within nonoperating allowable flight temperature limits during spacecraft fault conditions. The design of the CIRAS focal plane mount for flight use is complete at this time and involves mounting the HOT-BIRD detector on a detector pallet with cables and a cold shield, which will in turn be mounted on a detector mount (see Fig. 4). The detector mount attaches directly to the optics housing via a low-conductance support. A lightweight, flexible thermal strap attaches the detector to the cold tip of the cryocooler to eliminate concerns regarding misalignment and jitter due to the cryocooler's cold-tip vibration. The thermal strap will be configured with a heater to allow outgassing of the FPA in the event of icing contamination in orbit.

E. CIRAS Brassboard Performance

A complete brassboard assembly consisting of the optics (telescope, collimator, spectrometer, imager), detector (mounted on the IDCA), and cryocooler was assembled, integrated, and tested, first in ambient and then in TVac, as shown in Fig. 9. In the brassboard configuration, the flight-like CIRAS optical assembly was integrated and aligned to the IDCA on a ground-support equipment (GSE) baseplate. The CIRAS optics are mounted atop flight-like thermal isolation bipods, and the IDCA is mounted on an adjustable bracket atop the GSE baseplate. The adjustable bracket provides articulation of the IDCA with respect to the fixed CIRAS optics. During ambient testing, the entire optomechanical assembly, comprising telescope/spectrometer, IDCA, baseplate, and subplate, was mounted on a two-axis gimbal, which allowed the assembly to be rotated in azimuth over the 15.4° FOV of the CIRAS entrance slit. In TVac, a large pointing mirror is used to direct the beam to multiple sources, including three blackbodies in the chamber, and through a window to the targets placed external to the chamber, including a collimator that projects a slit for spatial testing, an etalon, and a gas cell.

TABLE IV
KEY PERFORMANCE PARAMETERS REQUIRED AND OBSERVED FOR CIRAS IN THE MOST CHALLENGING "ZOOM" MODE

Performance Parameter	Req.	Meas.	Uncty.
Spatial Performance			
Orbit Altitude (km)	600.0	N/A	N/A
Min Spatial Field of View (deg)	15.4	15.4	0.1
Max Spatial Resolution (mr)	5.83	1.80	0.1
Max Spatial Sample Spacing (mr)	0.605	0.60	0.05
Spectral Performance			
Min Wavelength (μm)	4.08	4.04	0.05
Max Wavelength (μm)	5.13	5.12	0.05
Max Spectral Resolution (nm)	5.0	4.5-5.2	0.2
Max Spectral Distortion (pixels)	2	1.0	0.5
Min Channels (pixels)	625	640	1
Radiometric Performance			
Operability	0.95	0.97	0.02
Max NEdT @ 4.9 μm 280K (K)	0.35	0.20 est.	0.05

Results from testing of the CIRAS brassboard look excellent, meeting the key performance requirements of the system. Table IV shows the key parameters and the results obtained from testing while the instrument was in ambient. Spatial performance is met with considerable margin since the optical system is driven by the image quality needed to achieve the high spectral resolution. The spectral range covers the whole band with a spectral resolution ranging from 4.5 to 5.2 nm. Radiometric performance looks good with high operability and signal collection efficiency of the system. Assuming worst-case photon and thermal noise from the flight system, we expect to meet our NEdT in-flight for all operable channels. We expect 100% operability after binning pixels for zoom mode or greater spatial resolution for all regions except the gap between the filters. A more complete description of the test procedure and results is given in the literature [36].

A major benefit of having a large-format FPA for CIRAS and future grating IR sounders is that the spectral and spatial

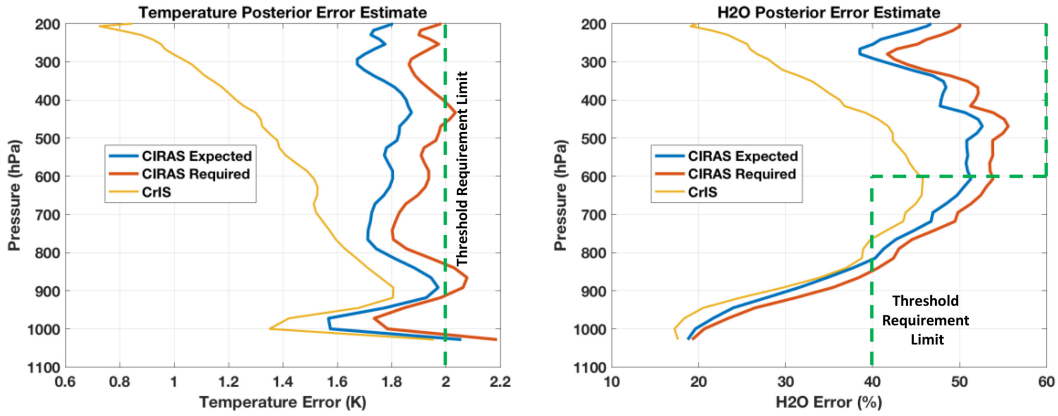

Fig. 10. (Left) Predicted temperature error for CIRAS expected and required, compared to CrIS. (Right) Water vapor error for CIRAS compared to CrIS.

sampling is better than Nyquist sampling. As shown in Fig. 5, the CIRAS spectral dimension is perpendicular to the spatial direction at the FPA. Misalignment of the dispersion direction of the grating relative to the rows in the FPA and smile and keystone distortions from the optics will produce spatial–spectral mixing if uncorrected. During preflight spectral testing and in-flight using the upwelling radiance, a transformation matrix can be generated that identifies the spectral and spatial positions of reference points in the FPA. This transformation matrix can then be used to resample the signals from each detector to a rectilinear spatial and spectral grid, allowing all spatial channels to have the same frequency grid. Simulations involving a 0.5° rotation resulted in radiometric errors of less than 250 mK in all channels [42]. Experience with the CIRAS brassboard has shown that we can achieve less than 0.1° (less than 1 pixel across the 640 dimension) in rotation accuracy and less than 2-pixel distortion, leading to even lower residual errors.

F. CIRAS Retrieval Sensitivity

To evaluate the impact of the CIRAS expected performance, compared to legacy sounders, a retrieval simulation for temperature and water vapor profiles was performed. The simulation considers both the "expected" capability (based on observed capability of the brassboard) and the "required" capability. The assumptions used in the model for the expected capability include an NEdT of 0.2 K at 280 K and a spectral resolution (FWHM of the SRF) of 4.5 nm. The "required" capability for CIRAS is introduced to reflect the current design capability with margin while still providing adequate sensitivity of retrieved temperature and water vapor accuracy. We establish a requirement of spectral resolution of 5 nm for all channels and NEdT at 280 K of $<$0.5 K for wavelengths less than 4.6 μm and $<$0.35 K for wavelengths greater than 4.6 μm.

Fig. 10 shows the results of the simulation for temperature (left) and water vapor profile (right) sensitivity based on the expected and required CIRAS instrument performance contrasted with the CrIS instrument. The error profiles were calculated by taking the square root of the diagonal of the posterior error covariance. This analysis uses simulated CIRAS SRFs and includes the NEdT as the only error term. An operational retrieval would have more error terms and could have higher errors. The results show compliance with the "Threshold" capability for temperature defined by NOAA [30], for most levels to 400 mb, allowing some margin for retrieval errors. Water vapor meets threshold requirements to 850 and 600–400 mb but does not between these levels. CrIS also appears to not meet the requirement in this region to a lesser extent, which may indicate a difference in assumptions between this analysis and that used to define the threshold requirements. Similar performance comparisons have been predicted independently for CIRAS, and despite the lower performance compared to CrIS, a positive forecast impact has been predicted when added to the operational system [32], [33]. The CIRAS far exceeds the threshold spatial resolution and coverage requirements, 50 km $\times$ 1100 km, as indicated in Table II in global mode, while having additional modes with higher spatial resolution.

IV. Next-Generation Technologies

In the following sections, we examine a few new technologies that will improve the number of spectral channels and spatial resolution in grating spectrometer IR sounders and extend the CIRAS approach to the VLWIR. These technologies include a concept for an optical system operating in the long-wavelength infrared (LWIR; λc $\sim$8 to 13 μm) as an example of how the next generation of optics can be made smaller. They also include technologies for LWIR and VLWIR detector materials and readouts and high-performance cryocoolers, all in the context for use on future grating spectrometer IR sounders, like MIRIS (for LEO) and SIRAS-G (for GEO).

A. Optics

Wide-field all-refractive grating spectrometer optical systems have been demonstrated in the MWIR and VLWIR, as mentioned above, and are not the limiting factor in the spectral resolution of the system. The number of spectral channels once limited by detector technology in a grating spectrometer can now be as many as can be placed on an FPA. 2 K or 3 K format FPAs are now available and can be placed under a single objective band, reducing the total number of spectrometers required in a future IR sounder to as few as two (e.g., MIRIS).

The new generation of IR sounder wide-field all-refractive grating spectrometer optical system could employ a more compact design than that used on CIRAS. An example is shown in Fig. 2 (top right) for an LWIR hyperspectral IR spectrometer for a composition sounder. The surfaces shown in red are nonspherical. This spectrometer is designed to operate in the 9.66–11.76 μm region with a spectral resolution of 5 nm to measure trace gas species and has 1280 spectral channels. The specific implementation is not important here but the optical form. The spectrometer operates near the Littrow condition, so the same optics can be used for collimating light from the slit and focusing light on the grating. The slit aperture is fabricated in black silicon or other darkened material to prevent scatter and stray light. Light passing through the slit is received by a rotationally symmetric spherical lens that focuses the pupil on the reflective stop on the rightmost surface of the dispersive element. The backside of the dispersive element is a free-form surface with a grating manufactured using e-beam lithography, like the immersion grating developed for CIRAS. With this approach, we realize a significant reduction in the number of elements and the overall size of the system. The resolving power of the immersed grating exceeds the resolving power of a planar grating of similar size by a factor equal to the refractive index ($\sim$4 for Ge). The technology exists to make immersion gratings on flat surfaces and first surface gratings on concave spherical surfaces. Combining them, as shown here, would further reduce the size of the systems.

B. IR Detectors

The next generation of grating IR sounders will depend on large-format long-wavelength cutoff IR detectors. IR sounders operate in the spectral band from 3.7 to 15.4 μm. HgCdTe IR detectors have proven successful over the years with cutoff wavelengths of up to 18 μm [43]. Single-element VLWIR HgCdTe detectors show high performance, whereas HgCdTe FPAs typically suffer from pixel-to-pixel nonuniformity and pixel operability issues. Some work has been done in characterizing a 15-μm cutoff HgCdTe mounted on a Hawaii-1RG ROIC operating at less than 25 K for astronomy applications [44], but operation at this temperature is not expected to be practical for operational IR sounders. Investments in VLWIR HgCdTe detector materials and FPAs are critical to reducing development time and risk of future flight IR sounder programs.

Type-II superlattice (T2SL) Barrier Infrared Detector (BIRD) technology [45]–[48], a breakthrough in III–V semiconductor-based IR detectors and FPAs, invented at JPL in recent years offers a solution for the realization of lower development cost while reducing dark current and improving uniformity and operability compared to II–VI material (HgCdTe). T2SL is an artificially engineered III–V semiconductor material capable of pervasive IR detection coverage, with an adjustable cutoff wavelength (λc) ranging from $\sim$2 to 15 μm and beyond. The T2SL-BIRD technology first saw success in the MWIR (λc $\sim$5.5 μm), demonstrating the best characteristics of both II–VI and III–V detectors: HgCdTe high operating temperature and InSb FPA uniformity, operability, large-format capability, and affordability. Specifically, the mid-wavelength high operating temperature (HOT) BIRD exhibits the same salient FPA characteristics as the market-leading InSb FPA, but at a 50K higher operating temperature [39], [40]. The CIRAS instrument baseline detector is T2SL since the MWIR material is mature and offers higher temperature performance at the 115 K operating temperature for hyperspectral imaging.

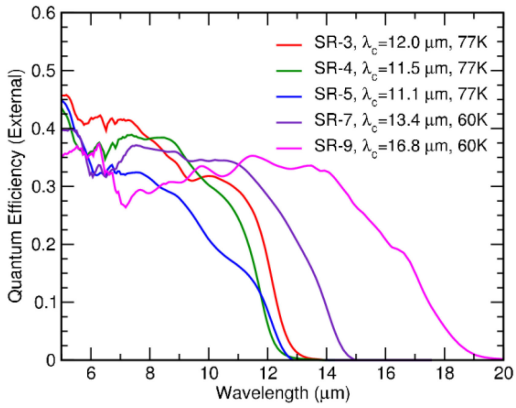

Fig. 11. QE for T2SL BIRDs with no antireflection coating.

The success of the mid-wavelength T2SL-BIRD has led to strong interest in the development of LWIR and VLWIR extensions. Ongoing LWIR T2SL-BIRD efforts have also demonstrated robust high operability/uniformity FPAs. A 12.6-μm cutoff FPA was developed for the NASA Sustainable Land Imaging—Technology (SLI-T) program. At 65 K, the FPA dark current density is 3×10^{-5} A/cm2, and the quantum efficiency (QE) is $\sim$18% in the LWIR (estimated internal detector QE, considering pixel fill factor and surface reflection, is $\sim$35%). The FPA demonstrated excellent uniformity and high NEDT operability (99.98%). The spectral dependence of the QE for several T2SL detectors manufactured at JPL is shown in Fig. 11.

C. Readout Integrated Circuits

Future grating IR sounders will require larger format FPAs to allow more spectral channels and smaller detectors to handle the high spatial resolution imaging requirement. Commercially available ROICs will meet these requirements. Aside from the analog ROICs, like the one used on CIRAS, the next generation of ROICs will use on-chip digitization to reduce noise, increase dynamic range, and increase readout rate.

For example, the Teledyne 2 K $\times$ 2 K GeoSnap, a digital output ROIC (DROIC), has a maximum frame rate of greater than 150 Hz and a full well of 2.2 Me- [49]. The device is extremely fast and has a high full well for an ROIC. The GeoSnap has low noise, like analog ROICs, with a read noise of 328 e–. This ROIC would be suitable for VLWIR sounding. Given a 16-μm cutoff detector, to enable sounding in the 15 μm CO_2 region, the detector must operate at 52 K, assuming Rule 07 performance [50], to prevent saturating this ROIC at the maximum frame rate. Higher frame rate and full well can be achieved from this device with small modifications in a semicustom fabrication. The use of an LVF in the grating spectrometer optical system is necessary

Fig. 12. (a) Northrop Grumman high efficiency cooler (HEC). (b) Northrop Grumman mini-cooler plus (MCP).

in the VLWIR to reduce background flux and prevent saturation of the DROIC, while also reducing noise and allowing a higher operating temperature of the optics.

An innovative approach to get around ROIC saturation is to use a Digital in-Pixel ROIC (DP-ROIC) [51], where the well capacitor is reset when filled, and a digital counter built into each unit cell is incremented; this provides a much higher effective well capacity than achievable in a conventional analog ROIC. A digital FPA made with a DP-ROIC permits longer integration times and higher photon flux and dark current, but it has higher read noise. The effective noise of the system is higher, so the advantage here is the ultimately higher operating temperature of the optics or cryocoolers or no need for the LVF filter, but a larger aperture may be required to recover the SNR. DP-ROICs can operate at kilohertz frame rates making them well suited for use in high spatial resolution LEO IR sounders.

DP-ROICs are at various stages of development. Currently available is the MIT-LL-13108 1280 $\times$ 480 format DP-ROIC with a 20-μm pitch and a maximum effective well depth of 98–426 million electrons (adjustable). This is approximately 16–70 times larger than the typical well depth in a conventional analog ROIC. A smaller version, the MIT LL-1398A DP-ROIC with 480 $\times$ 640 pixels on 20 μm centers, with identical properties has been selected for demonstration with the T2SL-BIRD at JPL supported by ESTO. The power dissipation of this device was not available at the time of this writing, but it is understood to be considerably higher than the analog ROICs or DROICs.

D. Cryocoolers

Cooler selection for future grating IR sounders requiring the VLWIR is highly dependent on the operating temperature of the FPA. For the next-generation IR sounder requiring 60 K operation, with the cryocooler's cold tip operating at approximately 5 K colder to account for the flexible thermal strap connecting them, the cold tip temperature would be set at 55 K. Assuming a 1 W heat lift, the radiator needed to dissipate heat from the cryocooler would be 0.18 m^2 and reject 87 W at a temperature of 298 K. The estimated 1 W thermal load for the FPA assumes an active load of the detector ($\sim$200 mW), the digital ROIC ($\sim$500 mW), and the structural conduction and radiated loads ($\sim$300 mW).

For these requirements, two good candidate choices for coolers are the Northrop Grumman High Efficiency Cooler (HEC) [see Fig. 12(a)], which has numerous coolers currently operating in space (TRL 9), and the smaller Northrop Grumman Minicooler Plus (MCP) [see Fig. 12(b)], which is currently in development (TRL 6). The MCP cooler is shown without structural/thermal supports. Assuming that the heat rejection for the coolers is 300 K, the bus power required to deliver 1 W of cooling for a 60 K FPA will be on the order of 50 W.

The cryocooler controller of choice is the IRIS LCCE-2 due to its efficiency, compact size, and cost. The LCCE-2 is a high-performance electronics box that provides command and control of a 100-W class cryocooler and is sufficiently radiation tolerant to support long-life space cryocoolers.

V. Benefits of Grating Spectrometers for Future IR Sounders

Although a variety of spectrometer instruments that would meet performance requirements can be conceived, the complexity of the development and the ultimate resource requirements of that instrument will impact the overall cost of a future flight operational program. Second-order artifacts will always exist that are particular to that design form, and it is hard to say that one form is better in every capacity. Resource utilization (i.e., size, mass, power, and data rate), however, is fundamental driver in instrument cost and can be used to compare different technical approaches to IR sounding.

A. Instrument Size and Mass

The size and mass of an IR instrument typically scale with the aperture diameter, not only because of the size of the telescope, but also because of the increase in size required by the on-board calibrators and scanning system. Grating spectrometers can use smaller collecting apertures to achieve the required NEdT since key noise sources are lower. The optical background flux and associated noise can be lowered in a grating spectrometer system through the use of bandpass filters (or an LVF) tailored across the FPA. Grating spectrometer instruments do not have correlated spectral noise and are less susceptible to vibrational noise [52], [53]. This is achieved by mounting the FPA directly to the optics, so the two move together under vibration, and the use of a flexible thermal link to the detector to further isolate the primary source of vibration in the system. Out of band response is limited through the selection of low orders (order 1 in CIRAS) and bandpass filters to reject optical ghosting.

Another key factor leading to a smaller aperture in grating spectrometers is a wide FOR with minimal off-axis spectral shift. As mentioned above, the greater the 2-D FOR of the optical system (and FPA size), the longer the dwell time, improving SNR that can be traded for a smaller aperture or better spatial and spectral resolution. AIRS acquires all spectral channels in a roughly circular 1.1° footprint on the ground in a dwell time of 22.4 ms [16]. The CrIS, an FTS instrument, can acquire all spectral channels in a 3° $\times$ 3° FOR (9 footprints) in 167 ms [2]. CIRAS acquires all spectral channels in a 15.4° $\times$ 1.1° FOR (12 footprints) in 257 ms, the longest of the three. CIRAS makes use of the increased dwell time by having only a 15-mm aperture (vs 3 mm in AIRS and 80 mm in CrIS) and warmer detectors (58 K for AIRS, 98 K for CrIS MWIR/SWIR, and 115 K for CIRAS). As the position of the detectors moves off-axis in the

FTS, the amount of spectral shift increases and the shape of the interferogram changes, often called self apodization. The effect is correctable but leaves residual noise in the spectra and increases the correlation of the noise in the entire band [54], [55]. Removing the spectral shift (keystone and smile distortion) in a grating system is achieved through a spatial resampling of the signals from the FPA as mentioned above, with minimal impact on the instrument noise [36].

B. Power and Data Rate

External data rates depend on spatial resolution, coverage, and number of spectral channels, whereas internal data rates of an FTS system are much higher. FTS systems must oversample the signal by over four orders of magnitude in order to make an interferogram that can be transformed into the spectrum [56], [57]. This leads to higher power consumption from the electronics in order to process the data stream (e.g., resampling, filtering, decimation, bit trimming, data compression). The mass and power of IRS in one early reference are 350 kg and 650 W, respectively, [58]. The grating spectrometer approaches mentioned above use much larger format FPAs, with much lower frame rates consistent with commercially available ROICs (e.g., the CIRAS frame rate is nominally 16.2 Hz). The reduced signal processing passes onto the ground system as well. Grating spectrometer IR sounders require a much simpler algorithm to calibrate the instrument in the Level 1B and Level 1C processing [19], [25] than the FTS [2].

C. Lifetime

Once built, a grating spectrometer optical system produces spectra continuously with no moving parts or power until it is obstructed or damaged. Advanced design and material technologies assure robustness of the assembly to launch, good thermal uniformity, and precision placement and bonding of the elements. Refractive optics can be sensitive to darkening due to radiation and contamination; however, these effects are less pronounced in the IR. All-refractive objective assemblies, like CIRAS but without a grating, were flown on the MODIS instruments [59] and have also provided good image quality with no apparent darkening for decades in space. The FTS system requires the use of at least one laser for metrology and a moving mirror mechanism. Although both of these subsystems have proven reliable to date, they increase the complexity, mass, and power of the instrument while reducing the reliability.

VI. Conclusion

The AIRS instrument was the first hyperspectral IR sounder in space designed for weather prediction and climate science. AIRS was also a technology demonstration of advanced IR optics (gratings, coatings, etc.), detectors, including long-wave cutoff HgCdTe, and active cryocoolers. The instrument has been an incredible success, performing exceptionally well over 20 years in space without a failure, and has shown exceptional resolution, stability, and accuracy. AIRS data have contributed to the improved weather forecast, validation of weather and climate models and processes, and measuring changes in climate and atmospheric composition over the last 20 years. The AIRS instrument is an engineering marvel, but it is limited due to the state of the art of detectors at the time, having only nearly linear ($2 \times N$) arrays. This led to residual coregistration errors, caused during the fabrication of the instrument, driven by the need to optically piece these arrays together to make a single spectrum. The use of these arrays led to detector outages since there are only two detectors per resolution element. These issues are relatively minor and have been resolved through ground processing algorithms in the Level 1C product.

New detector technology has changed the game for IR grating spectrometer sounders by providing more detectors per spatial resolution element and more spectral channels on a single FPA. This enables at or near 100% operability, with all channels under a single objective having nearly the same spatial and spectral response. The large-format FPA enables a higher signal collecting area, leading to smaller apertures or higher spatial resolution for a given aperture. These principles have been demonstrated in the CIRAS brassboard system built and tested at JPL sponsored by NASA ESTO, NOAA OPPA, and JPL internal investments. Results show that the CIRAS brassboard meets all key performance requirements within the uncertainty of the measurements and limitations of the testing. CIRAS provides the wide-field scan $\pm 50^\circ$ at legacy resolution, 14 km, and it also has a zoom mode to provide 3.5 km resolution over a smaller cross-track swath and a 1-km imaging mode. CIRAS operates in the MWIR band to fit in a CubeSat volume and meets most "threshold" requirements established by NOAA for an IR sounder to about 400 mb.

The lowest hanging fruit to improved weather forecast at a relatively low cost would be to fly one or two CIRAS-like instruments to "fill-in-the-gap" between crossings times of the POR and, in general, improve the temporal revisit of the constellation. This would benefit near real-time weather forecasting using IR sounding retrievals [60]. CIRAS Zoom mode enables higher horizontal resolution where needed, possibly closer to a storm or weather front. A constellation of CIRAS instruments could further improve temporal revisit and horizontal resolution of IR sounding measurements and potentially provide 3-D AMV wind measurements using 2–3 CubeSats or SmallSats in trailing orbits. The advantage of a large constellation over a single GEO sounder is the ability to provide global coverage with no loss of horizontal resolution in the polar regions. International and commercial participation in the global constellation would reduce cost and facilitate sustainability. Alternately, a single grating spectrometer IR sounder for GEO could use large-format FPAs and achieve a small aperture size and low mass, power, and data rate.

Regardless of orbital configuration or instrument type, the next generation of IR sounders promises to provide enhancements in spatial, temporal, and spectral resolutions. A strong and vibrant community of engineers and scientists has amassed a wealth of experience, techniques, and knowledge from AIRS, CIRAS, and the other operational sounders and are ready to handle the challenges we face in the utilization of new IR sounding data to improve the weather forecast and address the critical questions we face in the coming decade relating to weather, atmospheric composition, and climate science.

ACKNOWLEDGMENT

The authors would like to thank Tom Kampe and the team at Ball Aerospace for their development of the CIRAS optical system and Chris Wilson of Raytheon for performing retrieval simulations. The authors would also like to thank Brian Monacelli, Sir Don Rafol, Nick Tallarida, Hyung Cho, and Patricia Hansen of JPL and Megan Gibson of Sierra Lobo Inc. for their support in the integration and test of the CIRAS Brassboard; Fred O'Callaghan, George Aumann, Steve Broberg, and Evan Manning of JPL for their support in answering questions about the AIRS instrument; Dan Wilson for the development of the immersion grating; and Karl Yee for the development of the black silicon slit for CIRAS. This work was carried out at the Jet Propulsion Laboratory, California Institute of Technology.

REFERENCES

[1] M. T. Chahine *et al.*, "AIRS: Improving weather forecasting and providing new data on greenhouse gases," *Bull. Amer. Meteorol. Soc.*, vol. 87, no. 7, pp. 911–926, Jul. 2006, doi: 10.1175/BAMS-87-7-911.

[2] Y. Han *et al.*, "Suomi NPP CrIS measurements, sensor data record algorithm, calibration and validation activities, and record data quality," *J. Geophys. Res. Atmos.*, vol. 118, no. 22, pp. 12734–12748, Nov. 2013, doi: 10.1002/2013JD020344.

[3] P. Hébert *et al.*, "IASI instrument: Technical description and measured performances," in *Proc. 5th Int. Conf. Space Opt.*, Toulouse, France, Mar./Apr. 2004, vol. 10568, pp. 1056806-1–1056806-9, doi: 10.1117/12.2308007.

[4] F. Carminati *et al.*, "Assessment of the hyperspectral infrared atmospheric sounder (HIRAS)," *Remote Sens.*, vol. 11, no. 24, Dec. 2019, Art. no. 2950, doi: 10.3390/rs11242950.

[5] J. Yang *et al.*, "Introducing the new generation of Chinese geostationary weather satellites, Fengyun-4," *Bull. Amer. Meteorol. Soc.*, vol. 98, no. 8, pp. 1637–1658, Aug. 2017, doi: 10.1175/BAMS-D-16-0065.1.

[6] Y. M. Timofeyev *et al.*, "Hyperspectral infrared atmospheric sounder IKFS-2 on "Meteor-M" no. 2—Four years in orbit," *J. Quant. Spectrosc. Radiat. Transf.*, vol. 238, Nov. 2019, Art. no. 106579, doi: 10.1016/j.jqsrt.2019.106579.

[7] National Academies of Sciences, Engineering, and Medicine, *Thriving On Our Changing Planet: A Decadal Strategy for Earth Observation From Space*. Washington, DC, USA: National Acad. Press., 2017, doi: 10.17226/24938.

[8] National Oceanic and Atmospheric Administration, "NOAA satellite observing system architecture study, building a plan for NOAA's 21st century satellite observing system," Docket NOAA-NESDIS-2018-0053-NSOSA, May 2018. [Online]. Available: https://www.regulations.gov/document/NOAA-NESDIS-2018-0053-0002

[9] NOAA NESDIS, "Geostationary extended observations (GeoXO)," 2021. [Online]. Available: https://www.nesdis.noaa.gov/next-generation-satellites/geostationary-extended-observations-geoxo

[10] J. L. Marshall *et al.*, "Improving global analysis and forecasting with AIRS," *Bull. Amer. Meteorol. Soc.*, vol. 87, no. 7, pp. 891–894, Jul. 2006, doi: 10.1175/BAMS-87-7-891.

[11] A. E. Dessler *et al.*, "Water-vapor climate feedback inferred from climate fluctuations, 2003–2008," *Geophys. Res. Lett.*, vol. 35, no. 20, pp. 1–4, Oct. 2008, doi: 10.1029/2008GL035333.

[12] V. J. Realmuto *et al.*, "Plume tracker: Interactive mapping of volcanic sulfur dioxide emissions with high-performance radiative transfer modeling," *J. Volcanol. Geotherm. Res.*, vol. 327, pp. 55–69, Nov. 2016, doi: 10.1016/j.jvolgeores.2016.07.001.

[13] A. Behrangi *et al.*, "Early detection of drought onset using near surface temperature and humidity observed from space," *Int. J. Remote Sens.*, vol. 37, no. 16, pp. 3911–3923, Dec. 2015, doi: 10.1080/01431161.2016.1204478.

[14] A. Orr *et al.*, "Polar stratospheric clouds initiated by mountain waves in a global chemistry-climate model: A missing piece in fully modelling polar stratospheric ozone depletion," *Atmos. Chem. Phys.*, vol. 20, no. 21, pp. 12483–12497, Oct. 2020, doi: 10.5194/acp-20-12483-2020.

[15] J. Susskind *et al.*, "Recent global warming as confirmed by AIRS," *Environ. Res. Lett.*, vol. 14, no. 4, pp. 1–12, Apr. 2019, doi: 10.1088/1748-9326/aafd4e.

[16] P. Morse *et al.*, "Development and test of the atmospheric infrared sounder (AIRS) for the NASA earth observing system (EOS)," *Proc. SPIE*, vol. 3870, pp. 281–292, Jul. 1999, doi: 10.1117/12.373196.

[17] L. L. Strow *et al.*, "Validation of the atmospheric infrared sounder radiative transfer algorithm," *J. Geophys. Res. Atmos.*, vol. 111, no. D9, pp. 1–24, May 2006, doi: 10.1029/2005JD006146.

[18] R. G. Ross and J. I. Rodriguez, "Performance of the AIRS pulse tube coolers and instrument—A first year in space," in *Advances in Cryogenic Engineering*. New York, NY, USA: Amer. Inst. Phys., 2004, pp. 1293–1300, vol. 49B.

[19] T. S. Pagano, H. H. Aumann, D. E. Hagan, and K. Overoye, "Prelaunch and in-flight radiometric calibration of the atmospheric infrared sounder (AIRS)," *IEEE Trans. Geosci. Remote Sens.*, vol. 41, no. 2, pp. 265–273, Feb. 2003, doi: 10.1109/TGRS.2002.808324.

[20] L. L. Strow and S. DeSouza-Machado, "Establishment of AIRS climate-level radiometric stability using radiance anomaly retrievals of minor gases and SST," *Atmos. Meas. Techn. Discuss.*, vol. 13, no. 9, pp. 4619–4644, Aug. 2020, doi: 10.5194/amt-2019-504.

[21] H. H. Aumann *et al.*, "Radiometric stability in 16 years of AIRS hyperspectral infrared data," *Proc. SPIE*, vol. 10764, Aug. 2018, Art. no. 107640O, doi: 10.1117/12.2320727.

[22] T. S. Pagano *et al.*, "SI-traceability and measurement uncertainty of the atmospheric infrared sounder version 5 level 1B radiances," *Remote Sens.*, vol. 12, no. 8, Apr. 2020, Art. no. 1338, doi: 10.3390/rs12081338.

[23] T. S. Pagano *et al.*, "Performance status of the atmospheric infrared sounder ten years after launch," *Proc. SPIE*, vol. 8527, Nov. 2012, Art. no. 852703, doi: 10.1117/12.977309.

[24] W. L. Smith *et al.*, "Hyperspectral satellite radiance atmospheric profile information content and its dependence on spectrometer technology," *IEEE J. Sel. Topics Appl. Earth Observ. Remote Sens.*, vol. 14, pp. 4720–4736, May 2021, doi: 10.1109/JSTARS.2021.3073482.

[25] E. M. Manning *et al.*, "AIRS version 6.6 and version 7 level-1C products," *Proc. SPIE*, vol. 11127, Sep. 2019, Art. no. 1112718, doi: 10.1117/12.2529400.

[26] T. S. Pagano *et al.*, "Improving AIRS radiance spectra in high contrast scenes using MODIS," *Proc. SPIE*, vol. 9607, Aug. 2015, Art. no. 96070K, doi: 10.1117/12.2188311.

[27] T. S. Pagano *et al.*, "The spaceborne infrared atmospheric sounder (SIRAS) instrument incubator demonstration," in *Proc. Earth Sci. Technol. Conf.*, Aug. 2001, pp. 1–8. [Online]. Available: https://trs.jpl.nasa.gov/handle/2014/12938

[28] T. U. Kampe, "Application of spaceborne infrared atmospheric sounder for geosynchronous earth orbit (SIRAS-G) technology to future earth science missions," in *Proc. SPIE*, vol. 6966, Apr. 2008, doi: 10.1117/12.778050.

[29] T. S. Pagano *et al.*, "Requirements for a Moderate-resolution infrared imaging sounder (MIRIS)," *Proc. SPIE*, vol. 8870-7, Aug. 2013, Art. no. 887001, doi: 10.1117/12.2023813.

[30] NOAA NESDIS, "Low earth orbit (LEO) sounding satellite (SounderSat) concept exploration broad agency announcement," 2021. [Online]. Available: https://www.space.commerce.gov/business-with-noaa/future-noaa-satellite-architecture/

[31] T. S. Pagano *et al.*, "The CubeSat infrared atmospheric sounder (CIRAS), pathfinder for the earth observing nanosatellite-infrared (EON-IR)," in *Proc. AIAA/USU Conf. Small Satellites*, 2016, vol. SSC16-WK-32, [Online]. Available: http://digitalcommons.usu.edu/smallsat/2016/S8InstSciMis/1/

[32] Y. Zhou *et al.*, "Assessment of the CubeSat infrared atmospheric sounder impact on global numerical weather prediction using observational system simulation experiments," *J. Appl. Remote Sens.*, vol. 13, no. 3, 2019, Art. no. 032508, doi: 10.1117/1.JRS.13.032508.

[33] Z. Li *et al.*, "The alternative of CubeSat-based advanced infrared and microwave sounders for high impact weather forecasting," *Atmos. Ocean. Sci. Lett.*, vol. 12, no. 2, pp. 80–90, Jul. 2018, doi: 10.1080/16742834.2019.1568816.

[34] T. S. Pagano *et al.*, "CubeSat infrared atmospheric sounder technology development status," *J. Appl. Remote Sens.*, vol. 13, no. 3, Sep. 2019, Art. no. 032512, doi: 10.1117/1.JRS.13.032512.

[35] T. S. Pagano, "CubeSat infrared atmospheric sounder (CIRAS) NASA InVEST technology demonstration," *Proc. SPIE*, vol. 10177, May 2017, Art. no. 101770K, doi: 10.1117/12.2266282.

[36] T. S. Pagano *et al.*, "Ambient performance testing of the CubeSat infrared atmospheric sounder (CIRAS)," *Proc. SPIE*, vol. 11832, Aug. 2021, Art. no. 118320D, doi: 10.1117/12.2593625.

[37] W. McCarty *et al.*, "Observing system simulation experiments investigating atmospheric motion vectors and radiances from a constellation of 4–5-mm infrared sounders," *J. Atmos. Ocean. Technol.*, vol. 38, no. 2, pp. 331–347, 2021, doi: 10.1175/JTECH-D-20-0109.1.
[38] D. Santek *et al.*, "Feature-tracked 3D winds from satellite sounders: Derivation and impact in global models," in *Proc. 13th Int. Winds Workshop*, 2016, pp. 1–6. [Online]. Available: http://cimss.ssec.wisc.edu/iwwg/iww13/proceedings_iww13/papers/session7/IWW13_Session7_3_Santek_final.pdf
[39] D. Z. Ting *et al.*, "Mid-wavelength high operating temperature barrier infrared detector and focal plane array," *Appl. Phys. Lett.*, vol. 113, no. 2, May 2018, Art. no. 021101, doi: 10.1063/1.5033338.
[40] D. Z. Ting *et al.*, "InAs/InAsSb Type-II superlattice mid-wavelength infrared focal plane array with significantly higher operating temperature than InSb," *IEEE Photon. J.*, vol. 10, no. 6, Dec. 2018, Art. no. 6804106, doi: 10.1109/JPHOT.2018.2877632.
[41] D. Crisp *et al.*, "NASA orbiting carbon observatory: Measuring the column averaged carbon dioxide mole fraction from space," *J. Appl. Remote Sens.*, vol. 2, no. 1, Mar. 2008, Art. no. 023508, doi: 10.1117/1.2898457.
[42] T. S. Pagano *et al.*, "Electronic alignment for the CubeSat infrared atmospheric sounder (CIRAS)," *Proc. SPIE*, vol. 11131, Aug. 2019, Art. no. 111310H, doi: 10.1117/12.2530155.
[43] J. W. Beletic *et al.*, "Teledyne imaging sensors: Infrared imaging technologies for astronomy & civil space," *Proc. SPIE*, vol. 7021, 2008, Art. no. 70210H, doi: 10.1117/12.790382.
[44] M. S. Cabrera *et al.*, "Characterization of a 15-μm cutoff HgCdTe detector array for astronomy," *J. Astron. Telescopes, Instrum. Syst.*, vol. 6, no. 1, 2019, Art. no. 011004, doi: 10.1117/1.JATIS.6.1.011004.
[45] D. Z. Ting *et al.*, "Barrier infrared detector," U.S. Patent No. 8 217 480, 2012.
[46] D. Z. Ting *et al.*, "The emergence of InAs/InAsSb type-II strained layer superlattice barrier infrared detectors," *Proc. SPIE*, vol. 11002, May 2019, Art. no. 110020F, doi: 10.1117/12.2521093.
[47] D. Z. Ting *et al.*, "Development of InAs/InAsSb type II strained-layer superlattice unipolar barrier infrared detectors," *J. Electron. Mater.*, vol. 48, no. 10, pp. 6145–6151, 2019, doi: 10.1007/s11664-019-07255-x.
[48] D. Z. Ting *et al.*, "InAs/InAsSb type-II strained-layer superlattice infrared photodetectors," *Micromachines*, vol. 11, no. 11, 2020, Art. no. 958; doi: 10.3390/mi11110958.
[49] Teledyne Imaging Sensors, "GEOSNAP18_B0 ROIC technical manual," Feb. 13, 2020, 2020.
[50] W. E. Tennant, "'Rule07' revisited: Still a good heuristic predictor of p/n HgCdTe photodiode performance?," *J. Electron. Mater.*, vol. 39, pp. 1030–1035, 2010, doi: 10.1007/s11664-010-1084-9.
[51] K. I. Schultz *et al.*, "Digital-pixel focal plane array technology," *Lincoln Lab. J.*, vol. 20, no. 2, pp. 36–51, 2014. [Online]. Available: https://www.google.com/url?sa=t&rct=j&q=&esrc=s&source=web&cd=&ved=2ahUKEwjL1-b4ooL1AhWVl2oFHeCzDfAQFnoECAYQAQ&url=https%3A%2F%2Fwww.ll.mit.edu%2Fmedia%2F6166&usg=AOvVaw3aDqKjvZ_sU0uAcQeWeUVi
[52] S. Abdon *et al.*, "Meteosat third generation infrared sounder (MTG-IRS), interferometer and spectrometer test outcomes, demonstration of the new 3D metrology system efficiency," *Proc. SPIE*, vol. 11852, Jun. 2021, Art. no. 118521F, doi: 10.1117/12.2599240.
[53] V. Zavyalov *et al.*, "Noise performance of the CrIS instrument," *J. Geophys. Res. Atmos.*, vol. 118, pp. 13108–13120, 2013, doi: 10.1002/2013JD020457.
[54] Y. Han *et al.*, "Effect of self-apodization correction on cross-track infrared sounder radiance noise," *Appl. Opt.*, vol. 54, no. 34, 2015, pp. 10114–10122, doi: 10.1364/AO.54.010114.
[55] H. L. Huang *et al.*, "Geostationary imaging FTS (GIFTS) data processing: Measurement simulation and compression," in *Proc. SPIE*, Feb. 2001, vol. 4151, pp. 1–13, doi: 10.1117/12.416997.
[56] B. Fieque *et al.*, "Overview of space activity at SOFRADIR and new trends for future detector for science applications," *Proc. SPIE*, vol. 10562, 2016, Art. no. 105623Z, doi: 10.1117/12.2296086.
[57] R. J. Glumb *et al.*, "Development of the crosstrack infrared sounder (CrIS) sensor design," in *Proc. SPIE*, Feb. 2002, vol. 4486, pp. 411–424, doi: 10.1117/12.455124.
[58] D. Lamarre *et al.*, "Meteosat third generation: The infrared sounder instrument," *Imag. Appl. Opt.*, 2011, Art. no. JMA2, doi: 10.1364/FTS.2011.JMA2.
[59] T. S. Pagano *et al.*, "Development of the moderate-resolution imaging spectroradiometer (MODIS) protoflight model," in *Proc. SPIE*, Aug. 1996, vol. 2820-01, pp. 10–24, doi: 10.1117/12.258100.
[60] N. Smith and C. Barnet, "How forecasters use NUCAPS (JPSS soundings) in operational decision-making and anticipated benefits from geostationary orbit," Jul. 2018, doi: 10.13140/RG.2.2.36476.44165.

Thomas S. Pagano was born in Southern California, CA, USA, in 1960. He received the B.Sc. degree from the University of California at Santa Barbara, Santa Barbara, CA, USA, in 1982, and the M.Sc. degree from Montana State University, Bozeman, MT, USA, in 1984, both in physics.

He started his career with EG&G Energy Measurements, Goleta, CA, USA, testing electro-optic instrumentation for the Department of Energy. In 1985, he joined Hughes Aircraft Co. (now Raytheon), Goleta, CA, USA, as a Systems Engineer. He worked on studies for advanced imagers and sounders, including the interferometer thermal sounder study for the European Organisation for the Exploitation of Meteorological Satellites and the Moderate Resolution Imaging Spectroradiometer (MODIS) for NASA, Washington, D.C., USA. He then became the Chief Systems Engineer for the development of the MODIS instrument and retained that position through the delivery of the Protoflight unit to the Terra spacecraft. In 1997, he joined Caltech JPL as a Systems Engineer, and in 1999, he joined the AIRS project as the Calibration Team Leader. Since 2002, shortly after the launch, he has been the Project Manager for AIRS. He has authored or coauthored more than 60 conference and peer-reviewed publications relating to optical remote sensing instruments over his 35 year career in the field.

Mr. Pagano is a Fellow Member of the Society of Photo-Optical Instrumentation Engineers and assists in the organization and is the Chair of conferences relating to remote sensing, CubeSats, and SmallSats. He was the recipient of the NASA Exceptional Service Medal for Development of the AIRS Calibrated Spectra in 2004. He participates in the Global Space-based Intercalibration of Sensors working group. Since 2006, he has been a Member of the American Meteorological Society and has 4 U.S. patents.

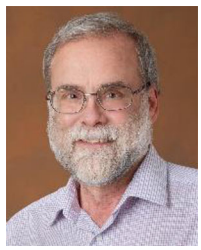

Dean L. Johnson received the M.S. and Ph.D. degrees in physics from Florida State University, Tallahassee, FL, USA, in 1975 and 1979, respectively.

He has 43 years of hands-on Cryogenics engineering experience with the Jet Propulsion Laboratory, Pasadena, CA, USA, working with Gifford–McMahon, Joule–Thomson, Stirling, and Pulse Tube cryocoolers for use with ground tracking antennas and airborne and space flight instruments. As a Cryogenics Engineer, he has developed various cryocooler integration technologies enabling cryocooler integration of microwave amplifiers and infrared and gamma-ray detectors for both laboratory test-bed and flight instrument programs. He is a Contract Technical Monitor for various cryocooler and cryocooler electronics development subcontracts. He has authored or coauthored more than 60 peer-reviewed papers covering topics in cryogenics and cryogenics-related research and development.

James P. McGuire received the B.Sc. M.Sc., and Ph.D. degrees in physics from the University of Alabama in Huntsville, Huntsville, AL, USA, in 1990.

From 1990 to 1996, he was a member of the Technical Staff with the Jet Propulsion Laboratory, Pasadena CA, USA, where he worked on the Wide Field/Planetary Camera 2 for the Hubble Space Telescope and several advanced concepts for astrophysics. From 1996 to 2012, he was with Optical Research Associates (now Synopsys), Pasadena CA, USA, where he provided optical engineering services, eventually rising to the position of Director of Optical Engineering Services. Since 2012, he has been with the Jet Propulsion Laboratory, where he has worked on advanced optical designs for planetary science, including Earth, Mars, other planets, Moons, and asteroids and astrophysics. He is currently the Deputy Manager of more than 100 people in the optics section. He has authored or coauthored more than 40 technical papers and 50 patents.

Dr. McGuire is a Member of SPIE and Optica (formerly OSA).

Mark A. Schwochert was born in Milwaukee, WI, USA, in 1964. He received the B.Sc. and M.Sc. degrees in mechanical engineering from California State University, Northridge, CA, USA, in 1987 and 1993, respectively.

He started his career with NASA's Jet Propulsion Laboratory (JPL), Pasadena, CA, USA, as a summer intern in 1986 and was hired full-time in 1987 after completing his undergraduate degree. He has more than 35 years of experience with JPL, developing flight instruments for science investigation and flight system engineering imaging. Flight instrument development activities include Soft X-ray Telescope Camera for Yohkoh, Wide Field and Planetary Camera II for Hubble Space Telescope, Imaging Science Subsystem for Cassini, Navigation Camera for Stardust, Science and Engineering Cameras for the Mars Exploration Rovers, Instrument for the Orbiting Carbon Observatory, Mars Color Cameras for Mars InSight, and SHERLOC Imaging Cameras for Mars 2020. His roles in projects include Cognizant Engineer, Instrument System Engineering, Integration and Test Lead, Project Element Manager, and Instrument Manager. He received the JPL Principal Engineer designation as an Imaging System expert in the areas of instrument system engineering and instrument integration and test. Since 2016, he has been the Supervisor of the Flight Instrument Detectors and Camera Systems Group.

Mr. Schwochert was the recipient of NASA, Washington, D.C., USA, Exceptional Medals in 2004 for the development of the Mars Exploration Rover Cameras and in 2015 for the development of the Orbiting Carbon Observatory-2 Instrument.

David Z. Ting (Senior Member, IEEE) received the B.S. degree (Hons.) from the California Institute of Technology, Pasadena, CA, USA, in 1980, and the M.S. and Ph.D. degrees from the University of Illinois at Urbana-Champaign, Champaign, IL, USA, in 1981 and 1986, respectively, all in physics.

He was a Senior Research Fellow with the Department of Applied Physics, Caltech, Pasadena, CA, USA. In 1995, he was an Associate Professor of physics with National Tsing Hua University, Hsinchu, Taiwan. In 1998, he joined the NASA's Jet Propulsion Laboratory, Pasadena, CA, USA, where he is currently a Senior Research Scientist, a Principal Member of the engineering staff, and the Deputy Director of the Center for Infrared Photodetectors, Pasadena, CA, USA. The results of his work have been reported in more 280 research publications and in more than 180 conference presentations and technical seminars. He holds 16 patents. His research interests include the studies of electronic and optical properties of semiconductors, quantum transport in tunnel devices and nanostructures, spintronics, and infrared photodetectors.

Dr. Ting is a Fellow of the SPIE. He was a 2018–2019 IEEE Photonic Society Distinguished Lecturer. He was the recipient of the NASA Exceptional Technology Achievement Medal in 2014 for his contribution and leadership in the invention and implementation of advanced infrared detector technology for space and terrestrial applications.